

Multiphase flow and tromp curve simulation of dense medium cyclones using Computational Fluid Dynamics

A. Farzanegan^{1*}, M. Gholami², M.H. Rahimyan³

1. Associate Prof., School of Mining Engineering, University College of Engineering, University of Tehran, Tehran, Iran

2. M.Sc. Student, School of Mining Engineering, University College of Engineering, University of Tehran, Tehran, Iran

3. Associate Prof., School of Mechanical Engineering, University College of Engineering, University of Tehran, Tehran, Iran

Received 27 February 2012; received in revised form 1 June 2013; accepted 10 June 2013

*Corresponding author: farzanegan@ut.ac.ir (A. Farzanegan).

Abstract

Dense Medium Cyclone (DMC) is a high capacity device widely used in coal preparation. Although this device is simple in design, the swirling turbulent flow, the presence of medium and coal with different density and size fraction and the presence of the air core make the flow pattern in DMCs complex. In this article the flow pattern simulation of DMC was performed with computational fluid dynamics (CFD) and Fluent software. Simulations were performed to give the axial velocity profile and the air core. Multiphase simulations (air/water/medium) were carried out with Reynolds Stress Model to predict turbulence dispersion, Volume of Fluid model to achieve interface between air and water phases, Mixture model to give multiphase simulation and Discrete Phase Model to predict coal particle tracking and tromp (partition) curve. The numerical results were compared with previously reported experimental data by Subramanian and close agreement was observed. In addition, separation efficiency of DMC was predicted using CFD simulations and shown by the Tromp curve. The comparison of simulated and measured Tromp curves showed that CFD simulation can predict Tromp curve reasonably within acceptable tolerance, however, for more accurate multiphase simulation including solid phase, Discrete Element Modeling (DEM) approach coupled with CFD was suggested. Through this research, it was found that characterization of mineral separation efficiency in DMCs based on Tromp curve concept can be done by CFD numerical simulation, which is very helpful in process optimization studies.

Keywords: Dense medium cyclone, gravity coal preparation, multiphase modeling, Tromp curve.

1. Introduction

Hydrocyclones, first developed in the 1950s, have found extensive use in mineral and chemical industries due to their simple design, operational simplicity, good performance and high capacity [1]. Dense medium cyclones (DMCs) have been used for accurate separation of particles of different densities. The DMC is a piece of equipment which utilizes fluid pressure energy to create rotational fluid motion. This rotational motion causes relative movement of the materials suspended in the fluid, thus permitting separation of these materials from one another. The rotational motion of the fluid is produced by tangential injection of the fluid into the cyclone.

The raw coal to be treated is suspended in a very fine medium, normally finely ground magnetite, and this pulp is fed tangentially into the cyclone through the inlet to a short cylindrical section. Solids separation is made in the cone-shaped part of the cyclone. The discard portion of the raw coal (sinks) leaves the cyclone at the spigot, and the clean coal (floats) via the vortex finder. The cylindrical section of the cyclone can be extended by the introduction of a barrel section which effectively increases the residence time within the cyclone and can improve the sharpness of separation between the clean coals and discard. The separation process that occurs inside a

cyclone is thought to be driven by the centrifugal force acting radially outward and an inwardly acting drag force. The centrifugal force developed inside the cyclone accelerates the settling rate of the particles, thereby separating them according to specific gravity in the medium. Thus the more dense material is flung to the outer wall of the cyclone where the settling velocity is at its lowest and progresses downwards along the cyclone wall in a spiral flow pattern until it exits at the spigot in an umbrella shaped spray. At the spigot, a reverse vortex begins to form a low pressure zone (generally referred to as the air core [1]) flowing upwards along the axis of the cyclone, through the vortex finder and exits at the overflow. The less dense material, due to the action of the drag force, settles more slowly. This material is captured in the upward flow of the reverse vortex and exits through the overflow. The medium density at which the separation between more dense and less dense material occurs is called the cut point density. Invariably, there often is a percentage of the feed coal distribution which gets trapped in an envelope of zero velocity inside the cyclone where the centrifugal force equals the drag force. Such material has an equal chance of reporting either to the overflow or the underflow and is often termed near density material.

DMCs are the main devices of the modern coal preparation to upgrade run-of-mine coal in the 0.5-50 mm size range [2]. Centrifugal forces cause the refuse or high ash particles to move towards the wall, where the axial velocity points predominantly downward, and to discharge through the spigot [3]. The DMC and particles track are shown in Figure 1.

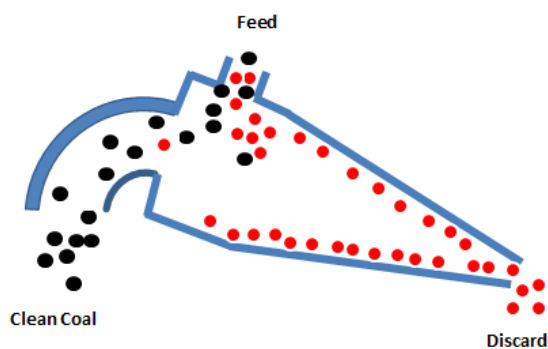


Figure 1. The DMC and different particles tracking

In order to simulate the fluid flow and particle dynamics, two considerations must be made: 1) selection of the appropriate model for turbulence

modeling; 2) selection of the appropriate model for multiphase modeling.

There is a large body of literature on CFD modeling of cyclone separators and many of these studies have used the Laser Doppler Anemometer (LDA) experiments of Hsieh (1986) to validate the modeling results. In this work, Hsieh has studied the single phase flow field in the cyclone with 75 mm in diameter to predict velocity profile, turbulence and particle relative velocity. In his work, turbulence viscosity modeled by the unidirectional Prandtl mixing-length model is given by [1]:

$$\mu_t = \rho l^2 \left[\frac{\mu_0}{\rho l^2} + \left| \frac{\partial v}{\partial r} - \frac{v}{r} \right| \right] \quad (1)$$

where, μ_t is the turbulence viscosity, μ_0 denotes the linear viscosity and l represents the Prandtl mixing length. The Navier-Stokes equations are solved using the Hopscotch method [1]. Most recent studies suggest that the turbulence in hydrocyclones is too anisotropic to treat with a k- ϵ model and at least a differential Reynolds stress turbulence model is needed to give reasonable velocity predictions [4, 5]. In his thesis, Suasnabar, calibrated the k- ϵ model to obtain correct velocity predictions in simulations of Hsieh's cyclone [6]. CFD can predict the flow field characteristics and particle trajectories inside a cyclone as well as the pressure drop. The standard k- ϵ model, RNG k- ϵ and realizable k- ϵ model were not optimized for strongly swirling flows seen in devices such as cyclones [7]. However, to reduce the computational cost the RNG, k- ϵ model can be used with about 12% deviation on experimental data [8]. The numerical studies carried out by Frederickson reveal that the RNG k- ϵ model underpredicts the variation of the axial velocity profile across the radial direction and over predicts the magnitude of the tangential velocity and the cyclone pressure drop [9]. Cortes [10] revealed that RNG model predictions are in good agreement with experimental measurements but Reynolds model provides better results. Lee [11] tested a number of turbulence models in his work and confirmed that only the second-order Reynolds stress model can give reasonable results for the flow velocity profile.

Recent CFD studies by Delgadillo and Rajamani [12] of Hsieh's cyclone have shown that the Differential Reynolds Stress Model (DSRM) still under-predicts the tangential velocities when used in conjunction with the Volume of Fluid (VOF) model to resolve the air core. Brennan [13] also

found that the Launder et al. (1975) DRSM under-predicted the tangential velocities in a CFD study of Hsieh's cyclone when used in conjunction with either VOF or mixture model to resolve the air core.

Recent advances in computational power have made Large Eddy Simulation (LES) model applicable for cyclone separators. Slack et al. [4] modeled single phase gas cyclones using LES and found good predictions of the velocities although the LES needed a grid of about 600,000 nodes compared to only 240,000 nodes for a DRSM simulation. This means that LES model generates more accurate predictions at the expense of need for more computational resources, i.e., memory and central processing unit execution time.

Flow pattern in DMC includes medium (usually magnetite) and coal particles dispersed in water. In addition, presence of the air core creates an interface between water and air. Therefore the flow in DMCs is a multiphase one. Davidson [14] used the mixture model in conjunction with a Reynolds averaged Navier-Stokes (RANS) based mixing length turbulence model to simulate concentrations profiles inside Kelsall's cyclone [15]. Comparison of Davidson's predictions with the later Gamma-Ray Tomography (GRT) density prediction of Subramanian [16] indicate that Davidson's simulations are qualitatively realistic. Suasnabar used both the full Eulerian approach with granular flow modeling and the mixture method to simulate the distribution and segregation of medium in 200 mm and 350 mm DSM pattern dense medium cyclones. Brennan [13] used the mixture model in conjunction with the DRSM turbulence model to simulate medium and the air core in a DSM pattern dense medium cyclone and the density predictions were compared to GRT data. He found that the Mixture model over-predicted medium segregation. The simulations also predicted that the highest concentration of medium was at the wall and that a film of pure water was predicted to occur just below the air core. Recently Delgadilo and Rajamani [18] and Wang [19] obtained the flow pattern and air core in hydrocyclones using RSM, LES and VOF models. Their results are appropriate references regarding flow pattern in DMCs.

The state of the art of numerical simulation of DMCs focuses on using a combined approach based on CFD and Discrete Element Method (DEM). Chu et. al. [20] studied the effect of the pressure at the vortex finder in DMCs using DEM model to describe the motion of discrete coal

particles, and CFD model to describe the motion of medium slurry which is a mixture of gas, water and fine magnetite particles. Similarly, Chu et. al. [21] studied flow dynamics and fluctuations in DMCs by CFD-DEM modeling. DEM applies Newton's equations of motion to every individual particle to simulate their movement. The traditional CFD solves the Navier–Stokes equations at a computational cell scale to simulate medium flow.

2. CFD approach

CFD is based on three equations describing mass conservation law, Newton's second law and energy conservation law. The general form of the mass conservation and momentum equations in the direction of x axis, also known as Navier-Stokes equations are:

$$\frac{D\rho}{Dt} + \rho \nabla \cdot \mathbf{v} = 0 \quad \text{or} \quad \frac{\partial \rho}{\partial t} + \nabla \cdot \rho \mathbf{v} = 0 \quad (2)$$

$$\rho \frac{Du}{Dt} = -\frac{\partial p}{\partial x} + \frac{\partial \tau_{xx}}{\partial x} + \frac{\partial \tau_{yx}}{\partial y} + \frac{\partial \tau_{zx}}{\partial z} + \rho f_x \quad (3)$$

where, ρ is the fluid density, \mathbf{v} represents the fluid velocity, p denotes the fluid pressure and $\frac{D\rho}{Dt}$ stands for the material derivative. In RANS method each variable is divided into two parts the average and the fluctuating. The averaged Navier-Stokes equations are given by:

$$\frac{\partial \rho}{\partial t} + \frac{\partial}{\partial x_i} (\rho u_i) = 0 \quad (4)$$

$$\frac{\partial}{\partial t} (\rho u_i) + \frac{\partial}{\partial x_j} (\rho u_i u_j) = -\frac{\partial p}{\partial x_i} + \frac{\partial}{\partial x_j} \left[\mu \left(\frac{\partial u_i}{\partial x_j} + \frac{\partial u_j}{\partial x_i} - \frac{2}{3} \delta_{ij} \frac{\partial u_k}{\partial x_k} \right) \right] + \frac{\partial}{\partial x_j} (-\rho \overline{u_i' u_j'}) \quad (5)$$

An additional term in this equation is $(-\rho \overline{u_i' u_j'})$. This term is due to the presence of turbulence in the flow that referred to the Reynolds stress statement. Therefore, solving the turbulence flow is solving Reynolds stress statement.

2.1. Turbulence models

2.1.1. The k-ε RNG model

Transfer equation for k-ε RNG model for k is:

$$\frac{\partial}{\partial t} (\rho k) + \frac{\partial}{\partial x_i} (\rho k u_i) = \frac{\partial}{\partial x_j} \left(\alpha_k \mu_{eff} \frac{\partial k}{\partial x_j} \right) + G_k + G_b - \rho \epsilon - Y_M + S_k \quad (6)$$

where, k is the turbulence kinetic energy, ϵ refers to the rate of dissipation, G_k represents the generation of turbulence kinetic energy due to the mean velocity gradients, G_b denotes the generation of turbulence kinetic energy due to buoyancy, Y_M stands for the contribution of the fluctuating dilatation in compressible turbulence to the overall dissipation rate, α_k is the turbulence Prandtl number for k and S_k user-defined source terms.

2.1.2. The Reynolds Stress model (RSM)

Transfer equation for RSM model is:

$$\begin{aligned} \frac{\partial}{\partial t}(\rho \langle \dot{U}_i \dot{U}_j \rangle) + \frac{\partial}{\partial x_k}(\rho u_k \langle \dot{U}_i \dot{U}_j \rangle) = \\ \frac{\partial}{\partial x_k} \left(\frac{\mu_i}{\sigma_k} \frac{\partial \langle \dot{U}_i \dot{U}_j \rangle}{\partial x_k} \right) + \frac{\partial}{\partial x_k} \left(\mu \frac{\partial \langle \dot{U}_i \dot{U}_j \rangle}{\partial x_k} \right) - \\ \rho \left(\langle \dot{U}_i \dot{U}_j \rangle \frac{\partial \langle U_j \rangle}{\partial x_k} + \langle \dot{U}_i \dot{U}_k \rangle \frac{\partial \langle U_j \rangle}{\partial x_k} \right) - \\ p \epsilon \end{aligned} \quad (7)$$

In this model, the equations are solved for each Reynolds stress component.

2.2. Multiphase modeling

2.2.1. The Volume of Fluid model (VOF)

The VOF model is a surface-tracking technique applied to a fixed Eulerian mesh. This model is designed for two or more immiscible fluids where the position of the interface between the fluids is of interest. In the VOF model, a single set of momentum equations is shared by the fluids, and the volume fraction of each of the fluids in each computational cell is tracked throughout the domain. The VOF formulation is based on the fact that two or more fluids do not interfere with each other. For each additional phase to the flow, there is a variable that is added in equations, i.e., the phase volume fraction in computational cell. The continuity equation for this model is given by:

$$\begin{aligned} \frac{1}{\rho_q} \left[\frac{\partial}{\partial t} (\partial_q \rho_q) + \nabla \cdot (\alpha_q \rho_q \vec{v}_q) \right] = S_{\alpha q} + \\ \sum_{\rho=1}^n (m_{pq} - m_{qp}) \end{aligned} \quad (8)$$

and momentum equation for this model is:

$$\frac{\partial}{\partial t}(\rho \vec{v}) + \nabla \cdot (\rho \vec{v} \vec{v}) = -\nabla p + \nabla \cdot [\mu(\nabla \vec{v} + \nabla \vec{v}^T)] + \rho \vec{g} + \vec{F} \quad (9)$$

2.2.2. The mixture model

The Mixture model is designed for two or more phases (fluid or particulate). The phases are treated as interpenetrating continua. The Mixture model solves for the mixture momentum equation and

prescribes relative velocities to describe the dispersed phases. The continuity equation for this model can be expressed as:

$$\begin{aligned} \frac{\partial}{\partial t}(\rho_m) + \nabla \cdot (\rho_m \vec{v}_m) \\ = 0 \end{aligned} \quad (10)$$

where, \vec{v}_m is the average velocity of mass and ρ_m represents the mixture density. Momentum equation for the mixture phase can be obtained by adding each equation separately. This equation is:

$$\begin{aligned} \frac{\partial}{\partial t}(\rho_m \vec{v}_m) + \nabla \cdot (\rho_m \vec{v}_m \vec{v}_m) = -\nabla p + \\ \nabla \cdot [\mu_m (\nabla \vec{v}_m + \nabla \vec{v}_m^T)] + \rho_m \vec{g} + \vec{F} + \\ \nabla \cdot \sum_{k=1}^n \alpha_k \rho_k \vec{v}_{dr,k} \vec{v}_{dr,k} \end{aligned} \quad (11)$$

where, μ_m for mixture phase is reduced to:

$$\begin{aligned} \mu_m \\ = \sum_{k=1}^n \alpha_k \mu_k \end{aligned} \quad (12)$$

2.2.3. Discrete Phase Model (DPM)

Coal particles are simulated using this model and its particle transfer equation is:

$$\begin{aligned} \frac{du_p}{dt} = F_D(u - u_p) + \frac{g_x(\rho_p - \rho)}{\rho_p} \\ + F_x \end{aligned} \quad (13)$$

where, $F_D(u - u_p)$ is the drag force on particle is, $\frac{g_x(\rho_p - \rho)}{\rho_p}$ represents the gravity force and F_x denotes the additional force (the pressure gradient force and the virtual mass force).

3. Simulation method

In this research, k-ε RNG and RSM methods were used to predict turbulence dispersion. The various models used are (a) VOF model to achieve interface between air and water phases, (b) Mixture model to give multiphase simulation and (c) DPM model to predict coal particle tracking and partition curve. Simulation process is shown in Figure 2.

4. Simulation Condition

For the purpose of model validation, the DMC used in Subramanian's experiments was used in this work. The geometry and mesh representation of the DMC and geometrical and mesh parameters are shown in Figure 3 and Table 1 respectively. The inlet type is tangential and the inlet shape is

square. The angle between the axis of the DMC and horizontal axis, i.e. the orientation angle, was set to 15°. The parameters used in the simulation are summarized in Table 2. Number of mesh applied in this work was 55,319 hexagonal cells

and the shape of coal particles was assumed to be spherical and mono-sized. Based on several trial simulations, it was found that meshing with hexagonal cells will generate the most accurate simulation results with suitable convergence.

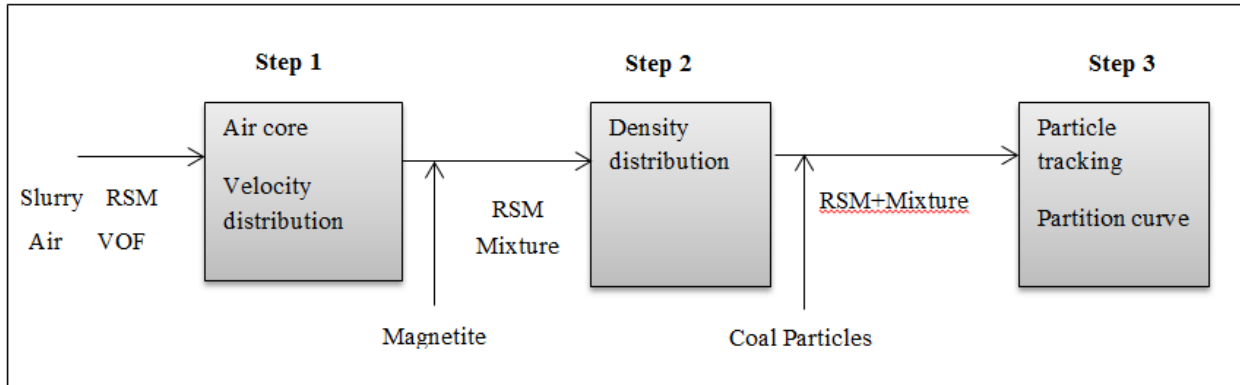


Figure 2. Simulation process applied in this work

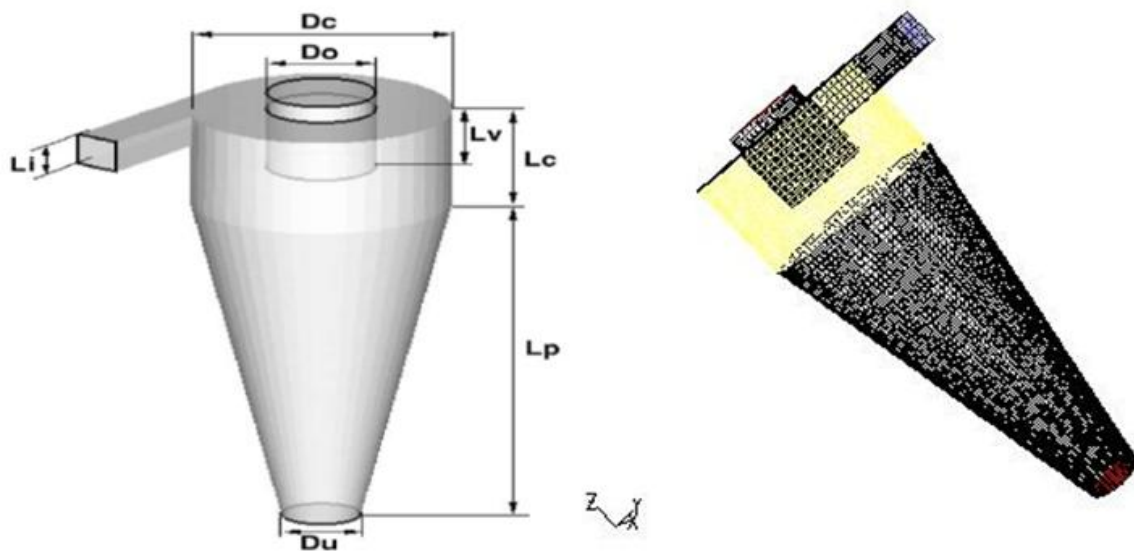


Figure 3. The geometry and mesh representation of the simulated DMC

Table 1. Geometry parameters of the DMC used for simulations

Parameter	Symbol	Value (mm)
Diameter of the body	D_c	350
Side length of inlet	L_i	65
Diameter of vortex finder	D_o	145
Diameter of spigot	D_u	105
Length of cylindrical part	L_c	200
Length of vortex finder	L_v	127
Length of conical part	L_p	695

Table 2. Parameters used in the model

Phase	Parameter	Symbol	Unit	Value
Solid	Density distribution	ρ	kg/m ³	1200 to 1800
	Particle diameter	d_i	mm	1,5,8,10 or 15
	Particle velocity at inlet	-	m/s	2.485
Gas	Density	ρ	kg/m ³	1.225
	Viscosity	μ	kg/m/s	1.8×10^{-5}
Water	Density	ρ	kg/m ³	998.2
	Viscosity	μ	kg/m/s	0.001
Magnetite	Velocity at inlet	-	m/s	2.485
	Density	ρ	kg/m ³	4945
	Sizes (and volume fraction)	-	μm	2(6%), 7(10%), 15(19%), 32(38%), 54(17%), 82(10%)
	Viscosity	μ	kg/m/s	3.3×10^{-3}
	Velocity at inlet	-	m/s	2.485
	Feed slurry density	-	kg/m ³	1467
	Pressure at vortex finder outlet	-	Pa	101,325
	Pressure at spigot outlet	-	Pa	101,325

5. Results and discussion

According to Figure 2, simulation process is as follows:

5.1. Step 1

In this step, RSM model was used to simulate turbulence and VOF model was used to obtain the air core. Static pressure contours are shown in Fig. 4. It can be seen from Figure 4 that the static pressure decreased radially from wall to center, and a low pressure zone is formed in the center. Contours of tangential velocity and axial velocity profile are shown in Figure 5. It is seen in Figure 4 that RSM model can simulate the air core in the DMC with high accuracy. Also in Figure 5, it can be seen that with moving away from the DMC wall to the center, the tangential velocity is reduced. In the wall area, the tangential velocity is negative and its quantity increases and then its value is positive. It means that the air rotational movement is in reverse direction compared with water rotation and moves upward.

2.5. Step 2

In this step, magnetite particles with different sizes and volume fractions as described in Table 1 were injected into the DMC. Size distribution of magnetite particles are shown in Figure 6. Magnetite particles viscosity is considered 3.3×10^{-3} [22]. In CFD simulation environment, Quick method setting was used to convert all equations to discrete form, PRESTO and SIMPLE settings were used for pressure and pressure velocity coupling, respectively. The equations were solved with the unsteady solver with a time step which

was typically 5.0×10^{-4} for the DRSM simulations. The density distribution simulated by CFD simulation is 1246.848 to 1247.156 kg/m³ and magnetite segregation is observable.

5.3. Step 3

There are two main approaches for modeling multiphase flows that account for the interactions between the phases. These are the Eulerian-Eulerian and the Eulerian-Lagrangian approaches. The former is based on the concept of interpenetrating continua, for which all the phases are treated as continuous media with properties analogous to those of a fluid. The Eulerian-Lagrangian approach adopts a continuum description for the liquid phase and tracks the discrete phase using Lagrangian Particle Trajectory (LPT) analysis. In the present study, one-way coupling method is used to solve the two phase flow and the Eulerian-Lagrangian approach is implemented for simulation of second discrete phase (particles). In this model, all fluid phases plus magnetite particles are the continuous phase and the particles are treated as the dispersed discrete phase. The particles motions are simulated by the Lagrangian trajectory analysis procedure. Forces acting on the dispersed phase include drag and gravity. The discrete phase equations are solved using Runge-Kutta method for particles. To calculate the trajectories of particles in the flow, the discrete phase model (DPM) was used to track individual particles through the continuum fluid.

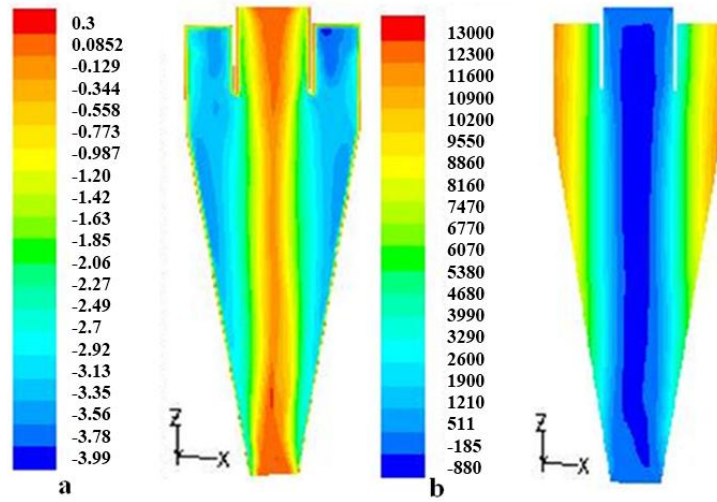


Figure 4. Static pressure contours (a) tangential velocity contour (b)

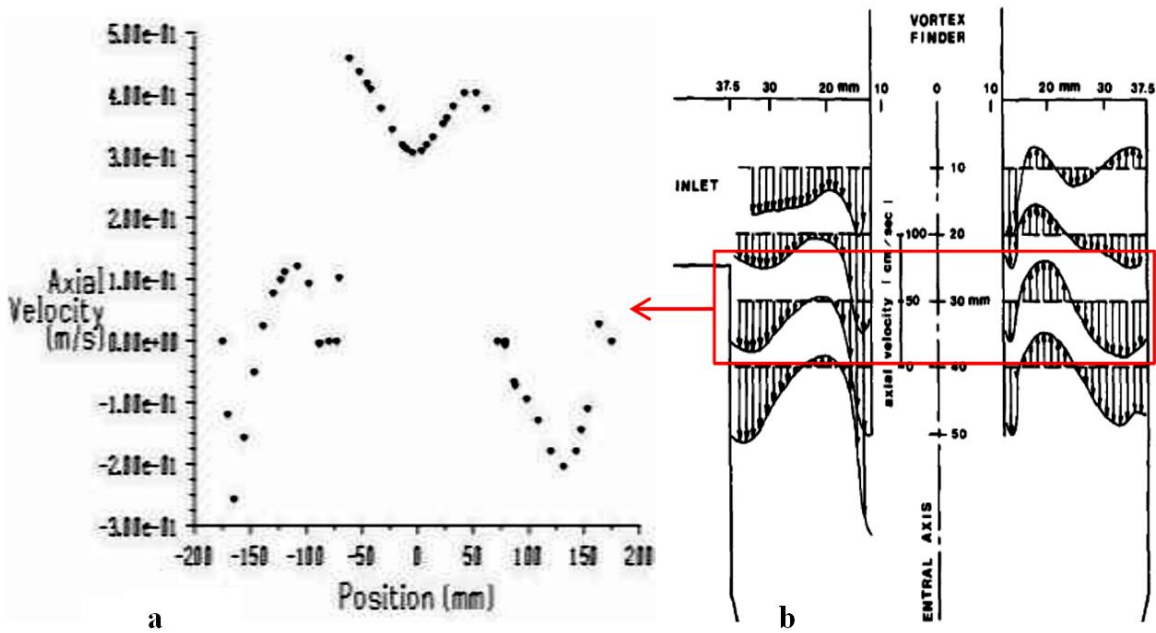


Figure 5. Axial velocity profile, (a) Simulated cyclone (b) Hsieh's cyclone [1]

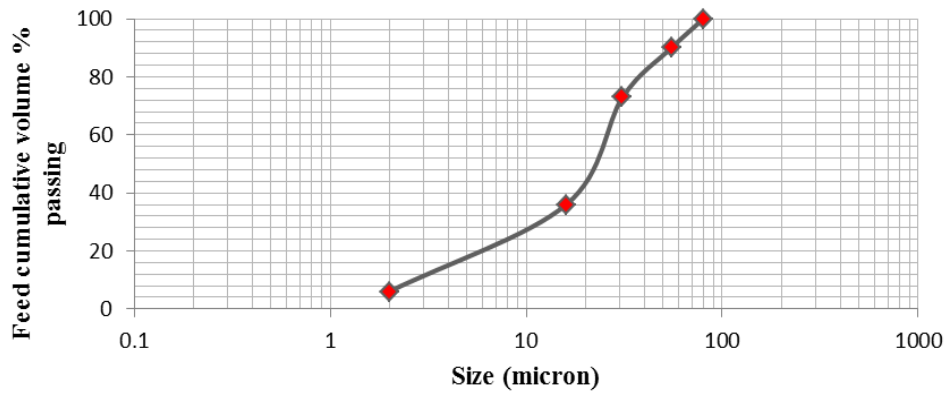


Figure 6. Feed magnetite size distribution used in CFD simulation

Particle diameters and their volume fractions are given in Table 3 For liquid sprays, a convenient representation of the droplet size distribution is the Rosin-Rammler expression. The complete range of sizes is divided into an adequate number of discrete intervals, each represented by a mean diameter for which trajectory calculations are performed. For the coal particles, the size distribution is of the Rosin-Rommler type, the mass fraction of droplets of diameter greater than d is given by:

$$Y_d = e^{-(d/\bar{d})^n} \tag{14}$$

where, the \bar{d} is the size constant and n is the size distribution parameter. Rosin-Rammler curve fit for the particles size is given in Figure 7. According to this figure, the \bar{d} value is 6.6 mm and the n value is 1.78. Simulation results are given in Figures 8 and 10.

According to Figure 9 the particle track is entirely consistent with the air core and the particles do not interfere with the air zone. The final result in the simulation is the partition curve. Separation efficiency in the DMC can be obtained from the partition curve. The particles were injected using a surface injection where 65 particles of 5-8 mm in size and different density were injected across the feed boundary using the instantaneous velocity field from a RSM/Mixture model simulation with medium at a particular feed relative density and feed head. Particle density distribution is 1200-1800 kg/m³. It can be seen that cut point density is 1450 kg/m³.

In Figure 10, a small deviation from experimental data is noticeable. This is due to the fact that the

LPT method is just suitable for dilute flow, since it only traces a single particle. Therefore, the effect of inter-particle interactions and the reaction of particles on the fluid are ignored which causes the deviation. In common coal preparation plants, the phase consisting of coal particles is greater than 10%. In recent years, the so-called combined approach of CFD and Discrete Element Method (CFD-DEM) has been developed and is able to account for particle-particle and particle-fluid interactions [3].

Table 3. Particles diameter and their volume fraction

Particles diameter	Volume fraction
0.25-1	0.05
1-5	0.4
5-8	0.26
8-10	0.11
10-15	0.15
15-25	0.03

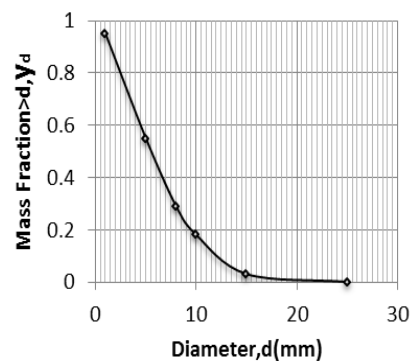


Figure 7. Rosin-Rammler curve fit for the particles size

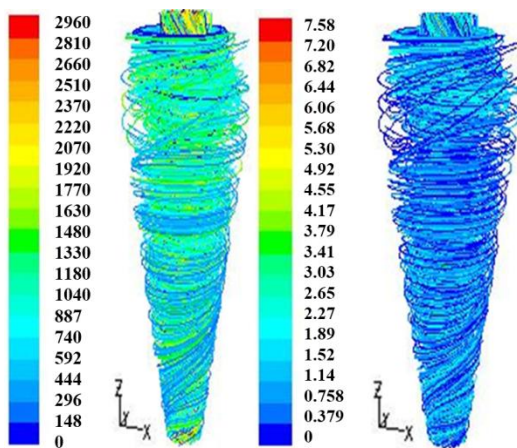


Figure 8. Particle tracks for a large number of particles at two different simulation times

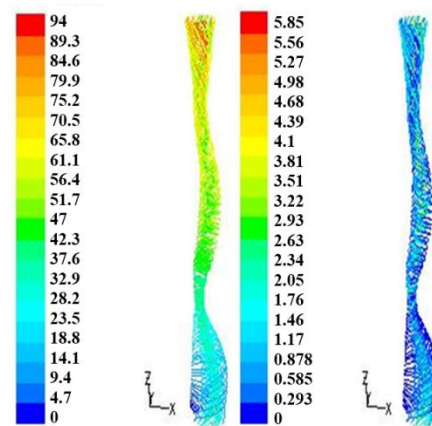


Figure 9. The shell that created with particles around the air core

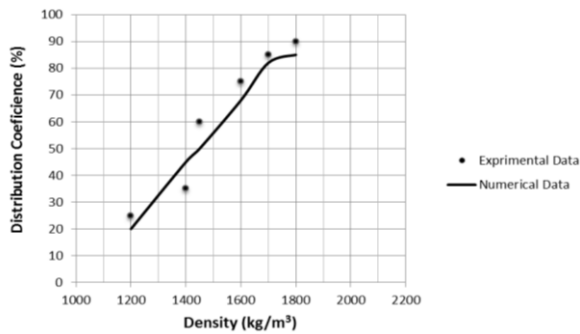


Figure 10. Predicted size-by-density partition curve for particles with 5-8 mm in size

6. Conclusions

RSM method is more effective in comparison with other $k-\epsilon$ methods for turbulence simulation. Both RSM and $k-\epsilon$ methods are appropriate in predicting axial and tangential velocities. VOF model is successful in modeling the two-phase flow and the air core which exists in the center of the DMC. Mixture model has been used in multiphase modeling and in this simulation density distribution varies from 1246.8 to 1247.2 kg/m^3 . The simulation time was two seconds and after five seconds, there is no change in magnetite layers. DPM method was used to simulate coal particles track. Discrete random walk model is an appropriate model in simulating particles distribution. Rosin-Rammler function was used to set up particle distribution in the simulations with determination of average particle diameter and particle mass fraction. The particle tracks are entirely consistent with the air core and the particles do not interfere with the air zone. The particles were injected using a surface injection where 65 particles of 5 to 8 mm in size and different densities were injected across the feed boundary using the instantaneous velocity field from a RSM/Mixture model simulation with medium at a particular feed relative density and feed head. Particle density distribution is 1200 to 1800 kg/m^3 . It can be seen that cut point density is 1450 kg/m^3 .

References

[1]. Hsieh K.T. and Rajamani, K., (1986). Phenomenological Model of the Hydrocyclone: Model Development and Verification for Single Phase Flow, *International Journal of Mineral Processing*. 22: 223-237.

[2]. Ishii M. and Mishima, K., (1984). Two-Fluid Model and Hydrodynamic Constitutive Relations, *Nuclear Engineering and Design*. 82: 107-126.

[3]. Chu, K.W., Wang, B. A. and Yu, A., (2009). CFD-DEM Modeling of Multiphase Flow in Dense Medium Cyclones. 193: 235-247.

[4]. Slack, M.D., Prasad, R. O., Bakker, A. and Boysan, F. (2000). *Advances in Cyclone Modeling Using Unstructured Grids*, Chemical Engineering Research and Design. 78: 1098-1104.

[5]. Suasnabar, D.J. (2000). *Dense Medium Cyclone Performance, Enhancements Via Computational Modeling of The Physical Process*, Ph.D. Thesis, University of New South Wales.

[6]. Narasimha, M., Brennan, M.S., Holtham, P.N. and Napier-Munn, T. J. (2006). *A Comprehensive CFD Model of Dense Medium Cyclone Performance*, Minerals Engineering. 20: 414-426.

[7]. Griffiths, W.D. and Boysan, F. (1996). *Computational Fluid Dynamics (CFD) and Empirical modeling of The Performance of A Number of Cyclone Samplers*, Aerosol Science. 27: 281-304.

[8]. Gimbun, J., Chuah, T. G., Fakhru'l-Razi, A. and Choong, Thomas S. Y. (2005). *The Influence of Temperature and Velocity on Cyclone Pressure Drop: A CFD study*, Chemical Engineering and Processing. 44: 7-12.

[9]. Frederickson, C. (2003). *Exploratory Experimental and Theoretical Studies of Cyclone Gasification of Wood Powder*, Doctoral thesis, Lulea University of Technology, Sweden.

[10]. Cortes, C. and Gil, A. (2007). *Modeling The Gas and Particle Flow Inside Cyclone Separators*, Progress in Energy and Combustion Science. 33: 409-452.

[11]. Lee, W.J., Yang, H., J. and Lee, Dong Y. (2006). *Effect of the cylinder shape of a Long-Coned Cyclone on the stable Flow-Field establishment*. 165: 30-38.

[12]. Delgadillo, J.A. and Rajamani, R. K. (2005). *A Comparative Study of Three Turbulence-Closure Models for the Hydro cyclone problem*. International Journal of Mineral Processing. 77: 217-230.

[13]. Brennan, M. S. (2006). *CFD Simulations of Hydro cyclones With an Air Core: Comparison between Large Eddy Simulations and A Second Moment Closure*, Chemical Engineering Research and Design. 84: 495-505.

[14]. Davidson, M. R. (1994). *A Numerical Model of Liquid-Solid Flow in A Hydro cyclone Separator With High Solids Fraction*, FED_Vol 185, Numerical Methods in Multiphase Flows, ASME, 29-39.

[15]. Kelsall, D.F. (1952). *A Study of the Motion of Solid Particles in A Hydraulic Cyclone*, Transactions of The Institution of Chemical Engineers. 30: 87-108.

[16]. Subramanian, V.J. (2002). *Measurement of Medium Segregation in The Dense Medium Cyclone Using Gamma-Ray Tomography*, Ph.D. Thesis, JKMR, University of Queensland.

- [17]. Davis, J.J., Wood, C.J. and Lyman, G.J. (1985). The Use of Density Tracer for the Determination of Dense Medium Cyclone Partition Characteristics, *Coal Preparation*. 2: 107-125.
- [18]. Delgadillo, J.A. and Rajamani, R. K. (2005). Hydro Cyclone Modeling: Large Eddy Simulation CFD Approach, *Mineral & Metallurgical Processing*. 22: 225-232.
- [19]. Wang, B., Chu, K. W. and Yu, A.B. (2007). Numerical Study of Particle-Fluid Flow in a Hydro Cyclone, *Industrial & Engineering Chemistry Research*. 46: 4695-4705.
- [20]. Chu, K.W., Wang, B., Yu, A. B., Vince, A. (2012). Particle Scale Modelling of the Multiphase Flow in a Dense Medium Cyclone: Effect of Vortex Finder Outlet Pressure, *Minerals Engineering*. 31: 46–58.
- [21]. Chu, K.W., Kuang, S.B., Yu, A.B., Vince, A. (2012). Particle Scale Modelling of the Multiphase Flow in A Dense Medium Cyclone: Effect of Fluctuation of Solids Flowrate, *Minerals Engineering*. 33: 34–45.
- [22]. Suasnabar, D.J. and Fletcher, C. A. J. (1999). A CFD Model For Dense Medium Cyclones, *Second International Conferene on CFD in the Minerals and Process Industries*, CSIRO, Melbourne, Australia.